

# Automatic Evaluation of Cancer Reduction During Radiotherapy

Valerio Bellandi<sup>1</sup>, Stefano Siccardi<sup>2</sup>

<sup>1</sup>Università Degli Studi di Milano, Department of Computer Science, Via Celoria 18, Milano, Italy

<sup>2</sup>Consorzio Interuniversitario Nazionale per l'Informatica, Via Ariosto, 25, Roma, Italy

## Abstract

In this study, we present an automated approach for monitoring tumor volume reduction during radiotherapy, aiming to optimize radiation dosing based on patient-specific responses. Conventional radiotherapy plans are static, often missing early and subtle volume changes detectable through imaging. Our proposed system compares planning CT scans with lower-resolution CBCT images acquired before each session, automatically delineating pathological structures and computing volume changes. If a variation higher than a predefined threshold is detected, an alert is issued for potential treatment adaptation. We developed and tested various image preprocessing and contour refinement methods, and introduced a supervised learning pipeline to (i) predict the presence of pathological structures and (ii) select the most appropriate contouring algorithm per case. Using synthetic data, we achieved promising classification performance and volume trend alignment with manual annotations. Future work will focus on real-patient data validation, inter-patient generalization, and algorithm fine-tuning to enhance adaptive radiotherapy decision-making.

## Keywords

Structure Segmentation, CBCT Analysis, Medical Image Processing, Machine Learning in Healthcare

## 1. Introduction

Radiotherapy is a cornerstone of cancer treatment, often administered in repeated sessions over several weeks. During this time, the pathological anatomy of a patient—particularly the volume and shape of tumors—can change remarkably. These changes may be due to therapeutic effectiveness, weight loss, organ motion, or other biological factors. However, traditional radiotherapy plans are defined at the outset based on a simulation CT scan, and they generally remain fixed throughout the treatment unless clinicians intervene manually. This static approach may lead to suboptimal outcomes, including unnecessary exposure of healthy tissue to radiation or insufficient dose to the tumor if important anatomical changes go undetected.

In current clinical practice, adaptation of the therapy plan is often based on visual inspection of pre-session images such as Cone Beam CT (CBCT) scans. While these provide useful anatomical information, visual inspection is inherently limited by human perceptual thresholds, time constraints, and inter-observer variability. Consequently, only large and easily observable changes are typically acted upon, while smaller but clinically relevant variations may be missed.

The aim of our research is to introduce an automated, data-driven system for monitoring tumor volume changes during radiotherapy. Our system compares pre-session CBCT images with the original planning CT scans, automatically detects and contours pathological structures, computes volume differences, and triggers alerts when changes exceed a configurable threshold. This alert mechanism enables clinical staff to reevaluate the treatment plan in a timely manner, potentially restarting the planning process to ensure optimal dosing.

To achieve this, we implement a multi-step image analysis pipeline that includes image preprocessing, structure segmentation within a defined Region of Interest (ROI), volume computation, and decision

---

*TADATA2025: The 4<sup>th</sup> Italian Conference on Big Data and Data Science, September 9–11, 2025, Turin, Italy*

\*Corresponding author.

<sup>†</sup>These authors contributed equally.

 valerio.bellandi@unimi.it (V. Bellandi); stefano.siccardi@unimi.it (S. Siccardi)

 0000-0003-4473-6258 (V. Bellandi); 0000-0002-6477-3876 (S. Siccardi)



© 2025 Copyright for this paper by its authors. Use permitted under Creative Commons License Attribution 4.0 International (CC BY 4.0).

logic based on thresholded volume variation. Beyond basic automation, we also integrate machine learning techniques to enhance the robustness of our system: we train classifiers to predict the presence of the target structure in each image slice and to select the best segmentation method for that specific context.

Our initial experiments using synthetic data demonstrate that automated monitoring can reliably track tumor regression trends and approximate manual annotations. These results suggest that such a system can serve as a valuable aid in offline adaptive radiotherapy, reducing the need for manual interventions while preserving patient safety and improving therapeutic precision.

In the following sections, we provide an overview of related work, describe the pipeline and learning-based enhancements, report experimental findings, and outline our plans for validating the approach on real patient data.

## 2. State of the Art

Research in **image processing in medicine** has a long history. For instance, a review of techniques for diagnostic imaging can be found in [1], that covers topics like the importance of image quality, analogue and digital image systems, image processing and analysis, 3D images and other. The important topic of image denoising with the objective to extract information about the scene being has been discussed e.g. in [2].

**Artificial Intelligence** applications for medical image processing has been used for image segmentation, to find specific structures or regions of interest; identification of abnormalities; enhancing the quality of medical images; tailoring treatment plans based on individual patient characteristics and response to therapy; predict disease progression, treatment response etc.; detecting artifacts in images; continuous monitoring of disease progression and treatment response over time, enabling timely adjustments to the treatment plan (see e.g. [3]). Many of these techniques have been used specifically in **radiation therapy**.

Several studies are devoted to tumor detection and segmentation, for instance see [4], [5] and [6] especially for liver cancer and metastases and [7] for a survey. These methods can be used at several stages of the patients' history, from cancer detection to treatment planning and evaluation of response to the therapy. The latter point introduces our focus: **adaptive radiotherapy**, that consists of adjusting treatment plans according to changes like organ deformation, weight loss, tumor shrinkage, and even biological changes, in order to reduce toxicity. It can be conducted in two ways: online (adjustments made during treatment sessions) and offline (adjustments made between treatment sessions), see e.g. [8] for an up to date review. The present study is in the field of offline adaptive radiotherapy.

## 3. The basic pipeline

In modern radiotherapy, patient treatment is carried out over multiple sessions, requiring careful planning, monitoring, and adaptation to anatomical changes. To support this process, a data processing pipeline is employed, which ensures that therapeutic plans remain accurate throughout the treatment cycle. The pipeline for a typical course of radiotherapy sessions is as follows:

1. During the planning session, a Computerized Tomography (CT) scan is performed. The contours of all relevant structures are manually delineated, and the therapeutic plan is defined.
2. The resulting images and identified structures are stored in the alert system; structure volumes are computed and saved.
3. Before each therapy session, a lower-resolution CT scan is performed.
4. These images are also stored in the alert system. Pathological structure contours are automatically detected, and the resulting volumes are compared with those obtained during the planning session.
5. If volume changes exceed a predefined threshold, an alert is issued, allowing the operator to review the situation and, if necessary, restart the process from step 1.

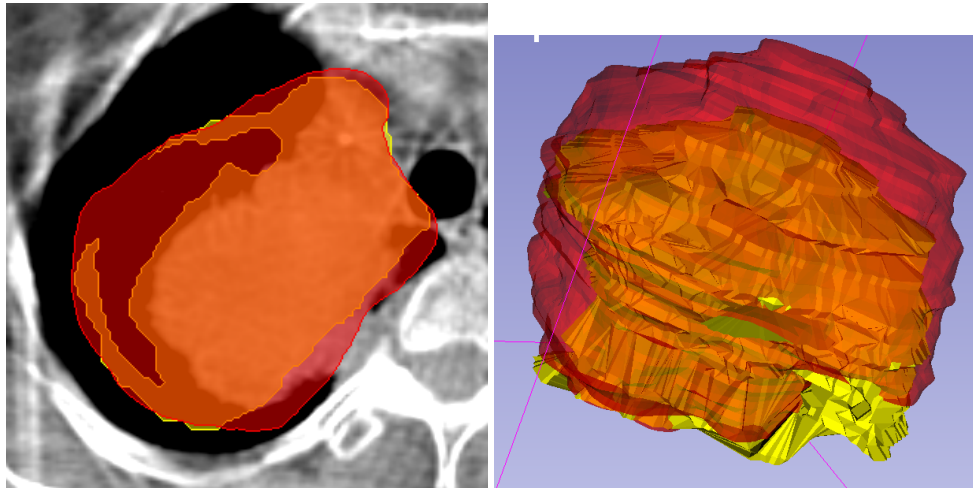


**Figure 1:** Example of a pathological structure's contours found during the planning session and automatically found during session 2. Left: a slice; right: 3D rendering

Steps 1 and 3 are already part of routine clinical practice. The CT scan in step 1 is called the *simulation* scan, while the CT scans in step 3 are called *CBCT* scans. CT devices save both images and structure contours to files in standard formats, most commonly DICOM<sup>1</sup>. These files can be processed using well-known open-source and proprietary tools. For example, we used 3D Slicer [9] and its SliceRT plugin [10], which is dedicated to Radiation Therapy, to prepare Fig. 1.

The devices also store, in the same format, information that allows CBCT scans to be aligned with the simulation scan, a process known as *registration*. This step is essential to ensure that structures from different sessions can be accurately compared.

Step 4 consists of identifying image contours based on grayscale differences. This task must be performed carefully, since multiple structures can appear in the same image. To address this, we define a Region of Interest (ROI), bounded by the structure contours identified during the planning session.

Several methods were tested to refine the contours, namely:

1. isotropically enlarging the ROI of some millimeter
2. smoothing the ROI
3. sharpening the ROI contrast
4. inverting the colours, to find dark structures like the lungs

At present, these methods have been tested on synthetic images; real patient data will be used in future work. Figure 1 (left panel) shows the contours of a pathological lung structure, with the outer red region representing the planning session contours and the inner yellow region representing the contours automatically detected during session 2 in a 2D CT slice. The corresponding 3D rendering of the structure is shown in the right panel.

In step 5, volumes are computed in the standard way: multiplying the structure area of each slice by the slice thickness for inner slices, and by half the slice thickness for the outer slices.

## 4. Refining the Structures

The described pipeline yielded promising results, as shown in fig. 2, left panel. In this case, the images were generated to simulate a patient showing large volume reduction for the pathological structure, so that the operators would decide to make two extra planning sessions to reduce doses at the 3rd and 17th sessions. The volumes found during the planning sessions (red line) are compared to those computed using automatically found contours for all the CBCT scans (blue line). It can be seen that there is agreement between the trends, however we noted that some points needed to be refined.

<sup>1</sup><https://www.dicomstandard.org/>

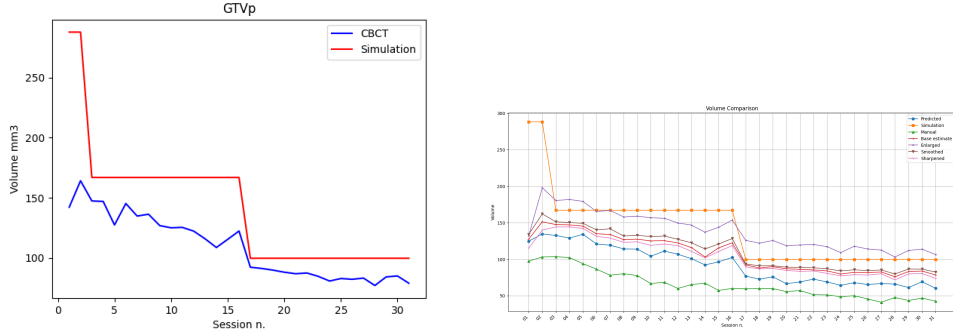


**Figure 2:** Pathological structure volume trend, as sessions progress. Left: base results (blue) compared to volumes found during the planning sessions (red). Right: comparison of algorithms, manual contours used for training and predicted after training.

First of all, the pathological structure may reduce even vertically; in such cases there are slices at some height with contours at planning time (simulation CT scan), where nothing must be found at therapy time. However, as we define the ROI boundary using contours of the simulation scan, the programs often erroneously find some contours.

Another point is that different algorithms yield different contours, each one with varying goodness of approximation depending of the images; we would like to have a way to choose the best suited algorithm for each case.

For this reasons, we decided to perform two learning procedure: the first one in order to create a model to check if a structure must be searched in a given image, the second one to choose the best suited algorithm to find its contours. We opted to have a supervised learning, with correct structures manually drawn in the CBCT images.

Fig. 2, right panel, shows the volume trends for:

1. the simulation scan contours (yellow line)
2. the contours found with each of the algorithms described above (base search for contours, enlarging the ROI 6 mm. in each direction, smoothing the image and sharpening it; we did not invert colours as the structure was not dark)
3. the manual contours drawn in the CBCT for learning (green line)
4. the contours drawn used the algorithms predicted by the learning model (blue)

It can be seen the advantage of the learning over the other methods.

We now describe the learning procedure.

We run all the algorithms for the CBCT images at vertical positions where a simulation contour could be found. This contour was used to define the ROI where the new contour should be found. If no manual contour existed for the CBCT image, we marked the image as *no contour*, otherwise as *contour*. This binary information was the target to predict for the first model.

In case of images with a manual contour  $m$ , we considered the region  $M$  delimited by it and, for each computed contour  $c$ , the delimited region  $C$ . Then we computed:

$$R_1 = \text{area}(M \cap C) / \text{area}(M); R_2 = 1 - \text{area}(C - M) / \text{area}(C) \quad (1)$$

so that  $R_1 = 1$  if the computed contour covers all the manual one and  $R_2 = 1$  if the computed contour does not cross the manual one. We used  $R = R_1 R_2$  as algorithm ranking to predict with the second model.

As features, we used a set of characteristics of the input image:

1. statistical metrics: mean, standard deviation (std), signal to noise ratio (mean/std), contrast  $((Max - min) / (Max + min))$
2. structural metrics: edge density (a measure of sharpness) and local variance (a texture measure)

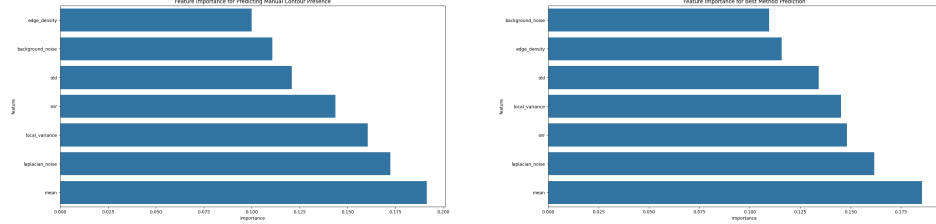


**Figure 3:** Estimated feature importance for the models. Left: prediction of the presence of a structure. Right: prediction of the best algorithm.

**Table 1**  
Performance for predicting presence of manual contour

	precision	recall	f1-score	support
not present	0.89	0.78	0.83	130
present	0.83	0.91	0.87	150
accuracy			0.85	280
macro avg	0.86	0.85	0.85	280
weighted avg	0.85	0.85	0.85	280

**Table 2**  
Performance for predicting best contouring method

	precision	recall	f1-score	support
enlarged	0.62	0.38	0.48	13
base	0.74	0.65	0.69	43
smoothing	0.76	0.94	0.84	93
sharpening	1.00	0.08	0.14	13
accuracy			0.75	162
macro avg	0.78	0.51	0.54	162
weighted avg	0.76	0.75	0.71	162

### 3. noise metrics: laplacian noise estimation and background noise estimation

The above metrics were computed for a rectangular region surrounding the ROI.

For these exploratory analysis, we used the 80% of data of our simulated patient to train a random forest classifier for each task, the remaining 20% for testing. We realized that the contrast feature had very low importance and dropped it.

Fig. 3 shows the estimated importance of features for both models; models performance indicators can be seen in tables 1 and 2.

The computed models were then applied to the whole set of images, to find an optimized structure. The result was used to compute the volumes shown in fig. 2, *predicted* line.

## 5. Conclusion and Future Work

This study presents a promising approach to enhancing radiotherapy through automated monitoring of tumor volume reduction using image analysis and machine learning techniques. By comparing planning CT scans with pre-session CBCT images, our system automatically detects and segments pathological structures, estimates volumetric changes, and generates alerts when above the established threshold deviations are observed. This enables clinicians to consider adaptive replanning more promptly and with greater precision.

Our preliminary results, based on synthetic data, show that the proposed pipeline can closely approximate manual contours and accurately track volume trends over multiple sessions. Furthermore,

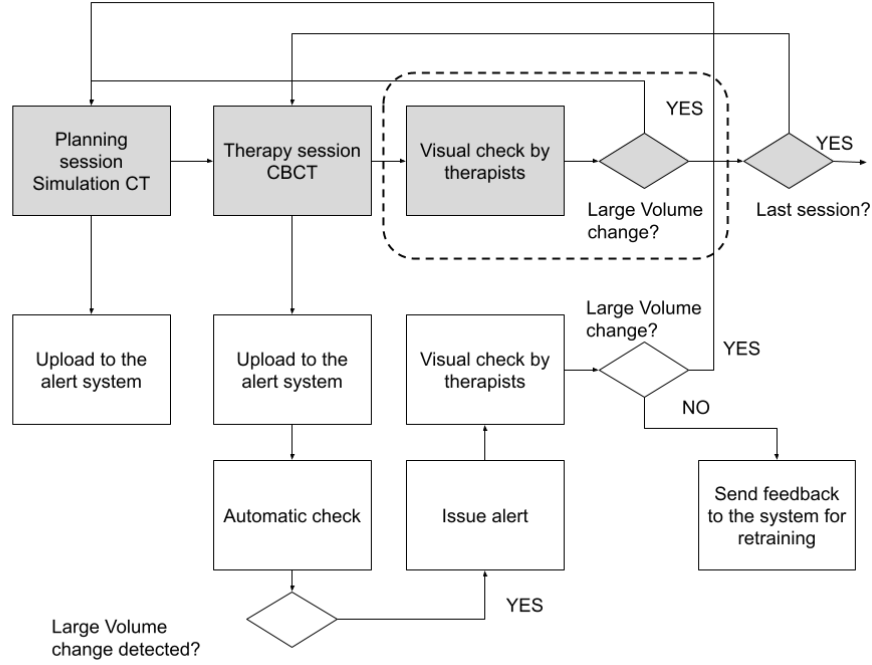


**Figure 4:** Workflow of the to-be online system.

the introduction of supervised learning models remarkably improves the system's ability to detect structure presence and select the most suitable segmentation method on a case-by-case basis.

Although the current findings are exploratory, they lay the groundwork for future development of a robust decision-support tool in offline adaptive radiotherapy. Moving forward, we plan to validate our system on real patient datasets, expand the training to include multiple patients for better generalization, and refine the image processing algorithms through parameter tuning and expert-guided ranking.

Ultimately, our goal is to support clinicians in delivering more personalized, responsive, and effective radiotherapy, reducing unnecessary radiation exposure and improving patient outcomes. The present work however exploratory has promising results. We plan to extend it in several directions:

1. we need to replicate the analysis for a suitable number of **real** patients
2. instead of using subsets of images of the same patient for training and testing, the algorithm should be trained on some patients and tested on others
3. we will extend the ranking based on areas (1) with a manual ranking by domain experts
4. we will extend the training to fine tune the algorithms

About the last point, we note that e.g. for smoothing we just used a bilateral filter with fixed parameters and for sharpening a 2D filter with a simple fixed kernel. For smoothing one might consider also blurring, gaussian blurring etc. moreover one might tune the parameters of each algorithm. The same applies for sharpening.

On the other side, we plan to implement an online system, that could be used by physicians of several hospitals, to routinely to get automated alerts when large changes are found in the patients' images. The system will be equipped with tools to upload images with or without manual contours, request contour detection and volume computation, review images and contours, get volume plots and reports and assign a rank to contours in order to retrain the models that choose the best algorithms. When a new CT scan will be uploaded, the system will automatically draw contours, recompute the volume and send an alert if it exceeds the defined thresholds. The physicians will visually review the images and decide if the therapeutic plan must be revised. The system is sketched in fig. 4. Gray boxes represent operations that are already performed in the normal practice. The dotted box encloses time consuming

manual checks, that might not be routinely performed; the system goal is to aid the therapists to check in depth only cases where a large volume changed is likely.

## Acknowledgments

This work is partially supported by i) the Università degli Studi di Milano within the program “Piano di sostegno alla ricerca”, ii) the MUSA – Multilayered Urban Sustainability Action – project, funded by the European Union – NextGenerationEU, under the National Recovery and Resilience Plan (NRRP) Mission 4 Component 2 Investment Line 1.5: Strenghtening of research structures and creation of R&D “innovation ecosystems”, set up of “territorial leaders in R&D, and iii) the project SERICS (PE00000014) under the MUR NRRP funded by the EU - NextGenerationEU.

## Declaration on Generative AI

The author(s) have not employed any Generative AI tools.

## References

- [1] K. Doi, Diagnostic imaging over the last 50 years: research and development in medical imaging science and technology, *Physics in Medicine & Biology* 51 (2006) R5. URL: <https://dx.doi.org/10.1088/0031-9155/51/13/R02>. doi:10.1088/0031-9155/51/13/R02.
- [2] N. Goel, A. Yadav, B. M. Singh, Medical image processing: A review, in: 2016 Second International Innovative Applications of Computational Intelligence on Power, Energy and Controls with their Impact on Humanity (CIPECH), 2016, pp. 57–62. doi:10.1109/CIPECH.2016.7918737.
- [3] R. Obuchowicz, M. Strzelecki, A. Piórkowski, Clinical applications of artificial intelligence in medical imaging and image processing—a review, *Cancers* 16 (2024). URL: <https://www.mdpi.com/journal/cancers>. doi:10.3390/cancers16101870.
- [4] G. Chlebus, A. Schenk, J. H. Moltz, B. van Ginneken, H. K. Hahn, H. Meine, Automatic liver tumor segmentation in ct with fully convolutional neural networks and object-based postprocessing, *Scientific Reports* 8 (2018) 15497. doi:10.1038/s41598-018-33860-7.
- [5] N. J. Wessdorp, J. M. Zeeuw, S. C. J. Postma, J. Roor, J. H. T. M. van Waesberghe, J. E. van den Bergh, I. M. Nota, S. Moos, R. Kemna, F. Vadakkumpadan, C. Ambrozic, S. van Dieren, M. J. van Amerongen, T. Chapelle, M. R. W. Engelbrecht, M. F. Gerhards, D. Grunhagen, T. M. van Gulik, J. J. Hermans, K. P. de Jong, J. M. Klaase, M. S. L. Liem, K. P. van Lienden, I. Q. Molenaar, G. Kazemier, Deep learning models for automatic tumor segmentation and total tumor volume assessment in patients with colorectal liver metastases, *European Radiology Experimental* 7 (2023) 75. doi:10.1186/s41747-023-00383-4.
- [6] M. Balaguer-Montero, A. Marcos Morales, M. Ligero, C. Zatse, D. Leiva, L. M. Atlagich, N. Staikoglou, C. Viaplana, C. Monreal, J. Mateo, J. Hernando, A. García-Álvarez, F. Salvà, J. Capdevila, E. Elez, R. Dienstmann, E. Garralda, R. Perez-Lopez, A ct-based deep learning-driven tool for automatic liver tumor detection and delineation in patients with cancer, *Cell Reports Medicine* 6 (2025) 102032. URL: <https://www.sciencedirect.com/science/article/pii/S2666379125001053>. doi:https://doi.org/10.1016/j.xcrm.2025.102032.
- [7] M. Z. Islam, R. A. Naqvi, A. Haider, H. S. Kim, Deep learning for automatic tumor lesions delineation and prognostic assessment in multi-modality pet/ct: A prospective survey, *Engineering Applications of Artificial Intelligence* 123 (2023) 106276. URL: <https://www.sciencedirect.com/science/article/pii/S0952197623004608>. doi:https://doi.org/10.1016/j.engappai.2023.106276.
- [8] O. M. Dona Lemus, M. Cao, B. Cai, M. Cummings, D. Zheng, Adaptive radiotherapy: Next-generation radiotherapy, *Cancers* 16 (2024). URL: <https://www.mdpi.com/2072-6694/16/6/1206>. doi:10.3390/cancers16061206.

- [9] A. Fedorov, R. Beichel, et al., 3d slicer as an image computing platform for the quantitative imaging network., *Magnetic Resonance Imaging* 30 (2012).
- [10] C. Pinter, A. Lasso, A. Wang, D. Jaffray, G. Fichtinger, Slicerrt: Radiation therapy research toolkit for 3d slicer, *Medical Physics* 39 (2012) 6332–6338. URL: <https://aapm.onlinelibrary.wiley.com/doi/10.1118/1.4754659>. doi:10.1118/1.4754659.